Ferrando-Rocher, M.; Herranz Herruzo, JI.; Valero-Nogueira, A.; Bernardo Clemente, B. (2018). Performance Assessment of Gap Waveguide Array Antennas: CNC Milling vs. 3D Printing. IEEE Antennas and Wireless Propagation Letters. 17(11):2056-2060. https://doi.org/10.1109/LAWP.2018.2833740

This article has been accepted for publication in a future issue of this journal, but has not been fully edited. Content may change prior to final publication. Citation information: DOI 10.1109/LAWP.2018.2833740, IEEE Antennas and Wireless Propagation Letters

Performance Assessment of Gap Waveguide Array Antennas: CNC Milling versus 3D Printing

Miguel Ferrando-Rocher, *Student Member, IEEE,* Jose I. Herranz-Herruzo, *Member, IEEE,* Alejandro Valero-Nogueira, *Member, IEEE,* Bernardo Bernardo-Clemente

***Abstract*—This paper focuses on comparing manufacturing features of 3D printing techniques versus conventional CNC milling in the context of Gap Waveguide Technology. To this end, a single-layer array antenna has been designed as a demonstrator. The antenna under test, intended for Ka band, is composed of 8×8 radiators fed by a gap-waveguide corporate network. Two identical prototypes have been manufactured, but each applying a different fabrication technique, i.e. 3D printing and CNC milling. The experimental results of both antennas are presented, under the same conditions and measurement facilities. The conclusions drawn in this paper pretends to provide a valuable assessment of 3D printing viability for gap waveguide arrays against the conventional milling technique.**

I. Introduction

A new generation of Ka-band satellites has recently been launched providing cellular coverage and significant improvement in transmission capacity [1]. In that context, satellites are expected to play an important role in the extension of 5G cellular networks to sea, air or remote land areas, where those systems cannot reach. Therefore, the massive adoption of new satellite communications on-the-move (SOTM) calls for low-profile terminals capable to be installed in ground vehicles or even airplanes. In addition to the defined electrical performance, hence, SOTM antennas must comply with demanding physical characteristics, mainly low profile and weight. Another essential variable for any massive application is obviously the fabrication cost. In this regard, additive manufacturing techniques can greatly contribute to reduce the weight and cost of SOTM antennas for ground terminals.

Gap waveguides (GW), firstly proposed in [2], have recently emerged as an alternative technology for mm-wave band devices. This full-metal technology enables an excellent shielding without resorting to a perfect electric contact between different parts of the device. The good performance, versatility, and relatively low manufacturing cost of this novel technology has attracted much attention in the last years. Gap waveguides hold their operation principle on a parallel-plate waveguide, where one of the plates is replaced by a high-impedance surface to create a cutoff condition. For that, the gap between the two plates must be less than a quarter wavelength. Commonly, the high-impedance condition is achieved through a bed of nails, a quarter wavelength in height at the center frequency.

Most devices in this technology are commonly constructed using CNC milling or, to a lesser extent, electrical discharge machining (EDM). Recently, the 3D printing boom has opened new avenues to exploration. Interestingly, scarce publications on GW technology designs using additive manufacturing (AM) can be found in the literature. Nevertheless, a very complete study comparing milling and 3D printing in terms of waveguide losses in transitions, power dividers or bends was recently released [3]. But the overall performance of a GW antenna was not covered there. Therefore, additive manufacturing procedures should be tested to check whether it can be a real alternative to the broadly used milling technique for GW antennas at Ka band. This paper addresses that issue by manufacturing and comparing two instances of one Ka-band GW array. The first prototype has been manufactured by stereolithography (SLA) followed by copper plating, while the second used a conventional milling process.

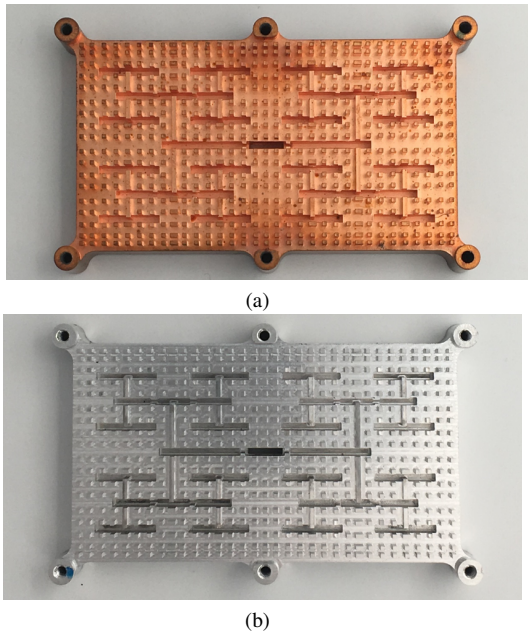

(a)

(b)

Fig. 1: Antenna prototypes. They are uncovered to clearly show the feeding network and cavities in GW technology. Both antennas are identical and share the same radiating layer. (a) Prototype 1: 3D printed. (b) Prototype 2: Machined aluminum.

The organization of this paper is as follows. Section II describes the GW array design. Section III presents the measurements of the manufactured prototypes and discloses the fabrication tolerances of both techniques. Section IV is devoted to assess the electrical array performance by comparing CNC milled versus 3D-printed prototypes. Finally, conclusions are drawn in Section V.

This article has been accepted for publication in a future issue of this journal, but has not been fully edited. Content may change prior to final publication. Citation information: DOI 10.1109/LAWP.2018.2833740, IEEE Antennas and Wireless Propagation Letters

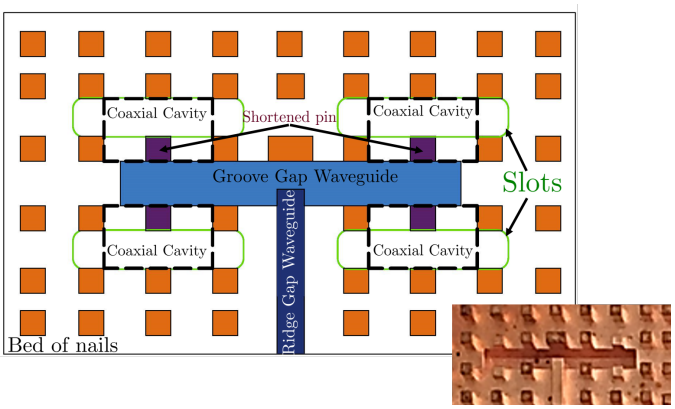

Fig. 2: Sketch of the basic radiating cell. The most significant parts are detailed. The slots, colored in green, are located above the coaxial cavities, framed in a black dashed line.

II. Antenna Design

The antenna chosen for this study is designed to operate at 30 GHz within a bandwidth around 2 GHz. It consists of a linearly-polarized slot array fed by a gap-waveguide corporate network. Each slot is backed by a coaxial cavity to enhance radiation. These cavities are created simply by shortening a center nail, which acts as the coaxial inner conductor. More design details can be found in [4] and will be omitted here for brevity. This particular antenna concept, comprising of nails with different heights, allows us to test the vertical accuracy of both manufacturing techniques. Except for the coaxial nails, whose height is 1.35 mm, the rest of them are 2.44 mm in height.

The array is subdivided into 4×4 basic cells. Each cell, in turn, is composed of 2×2 cavity-backed slots. Fig. 2 illustrates how each of these cells are fed. The feeding network uses a combination of ridge gap and groove gap waveguides to reach the cavities symmetrically. More details on the advantages of such ridge-groove combination can be found in [5]. Let us briefly mention that the TE_{10} mode in the groove gap waveguide is trapped into the coaxial cavity, providing full radiation from the slot with minimum reflected power.

Since 3D printing tolerances are known to be worse than those of conventional fabrication methods, a parametric study was carried out to evaluate the effect of manufacturing inaccuracies on the stopband of the bed of nails. Note that on this textured pattern relies the proper performance of the antenna. Typically, the most relevant parameters for the stopband design are the width and height of the nails and their periodicity. In this regard, the study focuses on the two first dimensions since nails periodicity is barely affected by manufacturing tolerances.

The worst possible scenario has been studied. A deviation of 500 microns has been considered, though the tolerances offered by the manufacturer are, at most, 100 microns in the worst case. This study of possible deviations in manufacturing is summarized in Fig. 3. Case A is the reference situation with no errors. It exhibits a 90% bandwidth for the stopband and the cut-off condition extends from 20 GHz to 53 GHz. In

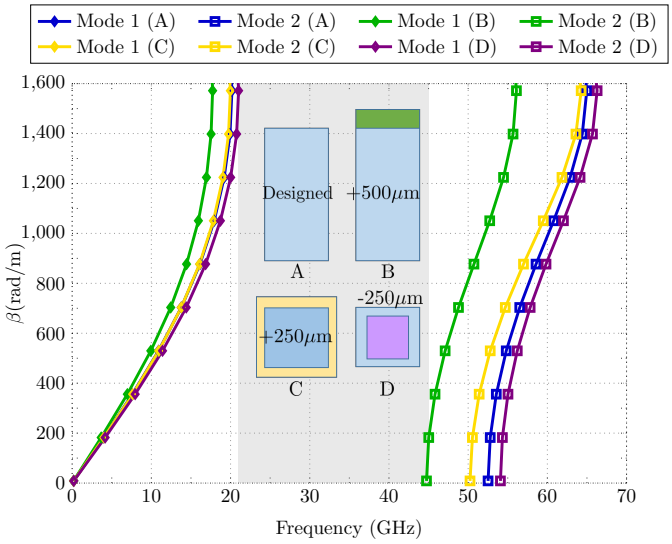

Fig. 3: Parametric study of the bed of nails. The deviation of the stopband is studied due to eventual manufacturing inaccuracies. (a) Designed nail. (b) 500 μm higher nail. (c) 250 μm thicker nail. (d) 250 μm thinner nail.

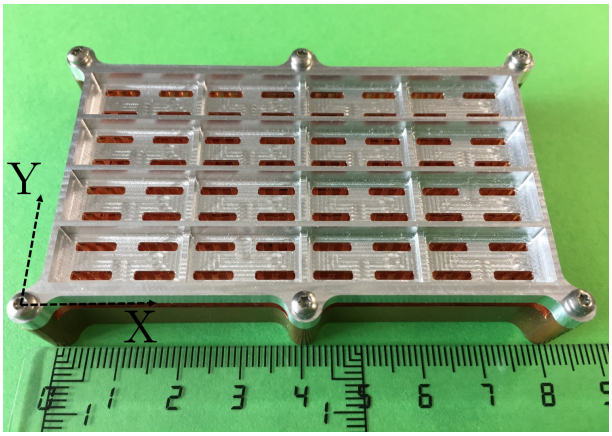

Fig. 4: Full manufactured antenna.

case B, a deviation of 500 microns in nail height is considered. Even in such unlikely case, mode 1 is not affected and mode 2 is shifted to a lower frequency, but still away from the working band. Next, possible deviations in nail width are studied. Case C corresponds to a nail whose side is 250 microns thicker than reference while in case D is 250 microns thinner. In none of these cases the inaccuracies altered the stopband frequency range substantially. This study reveals that 3D printing technique might be accurate enough for GW technology at Ka band in terms of bandgap performance, given its robustness against possible manufacturing inaccuracies.

Finally, in order to reduce the number of manufacturing variables and simplify the process, it was decided that both antennas would share the same radiating layer, being manufactured with a CNC milling machine. A set of optimized ribs have been included on the slots' plate to provide an enhanced rigidity to this layer, as it is shown in Fig. 4.

This article has been accepted for publication in a future issue of this journal, but has not been fully edited. Content may change prior to final publication. Citation information: DOI 10.1109/LAWP.2018.2833740, IEEE Antennas and Wireless Propagation Letters

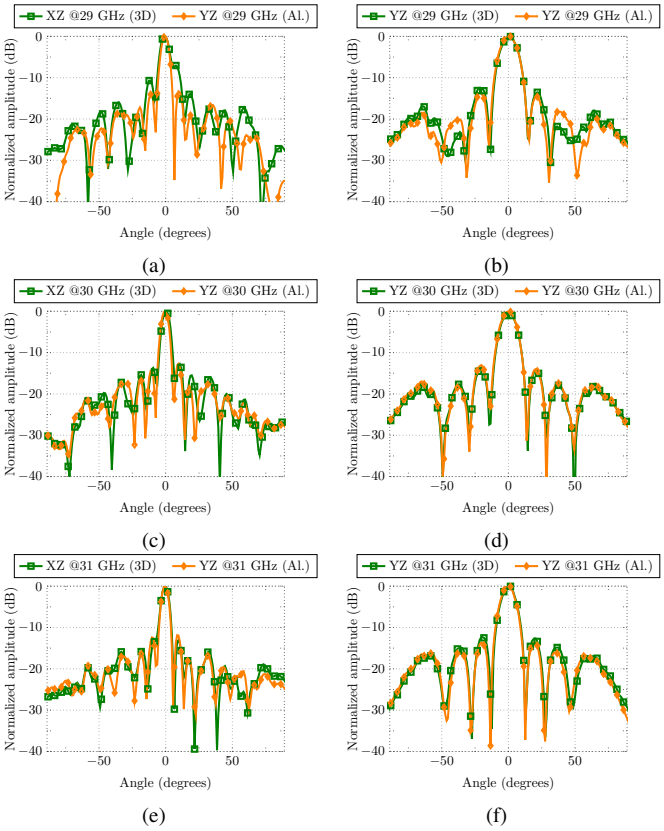

Fig. 5: Measured radiation patterns of both prototypes (aluminum and 3D-printed) at several frequencies: (a) H-plane at 29 GHz; (b) E-plane at 29 GHz; (c) H-plane at 30 GHz; (d) E-plane at 30 GHz; (e) H-plane at 31 GHz; (f) E-plane at 31 GHz.

III. Experimental Results

As explained above, the study presented here assesses the viability of additive manufacturing by comparing the electrical performance of two identical antennas constructed with different techniques. Both antennas are shown in Fig. 1 without the top plate. The first prototype has been manufactured using SLA printing followed by copper plating. SLA is a laser-based technology which uses a UV-sensitive liquid resin. A UV laser beam scans the surface of the resin and selectively hardens the material corresponding to the object's cross section, thus building the 3D body from the bottom up. The required supports for constructing overhangs and cavities are automatically generated and manually removed at the end of the process.

Once the solid object is built, it is subject to a metallic coating process, whose outcome is critical for the final electrical performance. In fact, techniques such as physical vapour deposition or electroplating, require access to every internal surfaces to correctly plate the structure [6]-[7]. As can be inspected in Fig. 1a, the targeted 3D structure was conceived to be free of intricate tunnels and allows a proper copper deposition by a straightforward procedure. The 3D-printed version was manufactured by Protolabs company. Conversely, the second prototype has been fully built inhouse by making use of the well-known CNC milling technique. This process

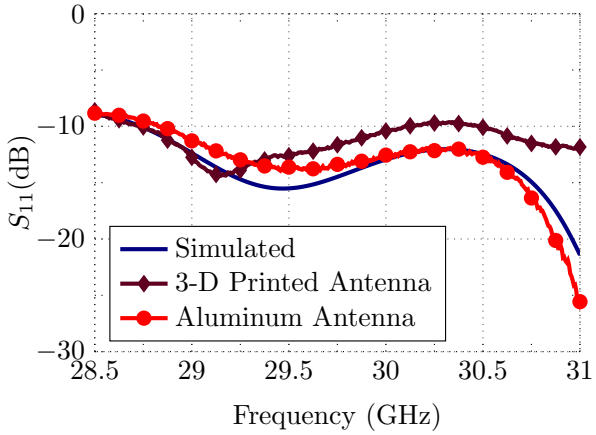

Fig. 6: Measured input reflection coefficient for both antennas.

TABLE I: Measured antenna parameters of 3D-printed prototype.

Frequency (GHz)	28.5	29	29.5	30	30.5	31
Directivity (dBi)	24.82	24.5	25.42	26.03	25.87	25.72
Gain (dBi)	23.96	23.89	24.45	25.55	25.15	24.58
Antenna Efficiency (%)	82.0	87.01	80.08	89.62	84.84	77.04

TABLE II: Measured antenna parameters of aluminum prototype.

Frequency (GHz)	28.5	29	29.5	30	30.5	31
Directivity (dBi)	25.39	25.58	25.85	26.09	26.24	26.22
Gain (dBi)	24.48	24.43	24.82	25.64	25.40	25.31
Antenna Efficiency (%)	81.17	76.74	78.89	90.02	82.26	81.08

requires a milling machine, aluminum material and several cutting bits, which must be equal to or smaller than the smallest feature of the desired pattern.

Both antennas have been measured under the same environment and during the same period of time, to avoid imbalances in the measurement equipment and calibration. The measured radiating parameters of both antennas are shown in Tables I and II. The mean efficiency is above 80% for both prototypes within the band of interest, being that of the 3D-printed version slightly higher. Recall that conductivity of copper is better than that of aluminum. Fig. 5 shows the radiation patterns in the main cuts (E and H plane) for several frequencies. In each subfigure the patterns of the 3D-printed and aluminum antennas, in green and yellow respectively, are compared. All the measured patterns present an overall good agreement, except for one visible discrepancy at 29 GHz in the H plane. Finally, the magnitude of the measured reflection coefficient is plotted in Fig. 6. A good agreement is shown between both experimental results, despite the aluminum version reveals a greater similarity to the simulated result.

A metrological study was carried out on both antennas to analyze the fabrication accuracy. The measured deviation from ideal dimensions of different constitutive parameters are shown in Table III. Predictably, the analysis of the tabulated data reveals that the mean manufacturing deviation committed by the milling technique is lower than that observed for the 3D-printed antenna.

This article has been accepted for publication in a future issue of this journal, but has not been fully edited. Content may change prior to final publication. Citation information: DOI 10.1109/LAWP.2018.2833740, IEEE Antennas and Wireless Propagation Letters

TABLE III: Metrological study of antenna dimensions.

Parameter	Designed (mm)	Mean deviation (μm)	
		Aluminum	3D printing
Groove width	1.6	7	37
Groove depth	3.473	13	33
Ridge width	0.986	13	14
Ridge height	1.548	41	44
Nail width	0.9	15	11
Nail height	2.439	3	9
Shortened-nail width	0.9	7	7
Shortened-nail height	1.35	12	23

IV. Discussion

A critic comparison of the experimental results and their connection to fabrication techniques are discussed next. The conclusions drawn in [3] will be taken as a reference, given the common points with this work.

Figs. 7b, 7d and 7f show three zoomed pictures of the 3D-printed antenna. Several imperfections in the sampled GGWs are evidenced. Such inaccuracies in the waveguides' walls were detected throughout the antenna. Conversely, those defects are not present in the aluminum piece, where the circular ripple left by the milling cutter is visible instead (see Figs. 7a, 7c and 7e). Such ripple, however, is merely one micron thick and its effect on electrical performance is negligible. One might state, therefore, that the overall fabrication quality of the aluminum antenna is notably better than that observed for the 3D-printed prototype. This fact contradicts to a certain extent what it is affirmed in [3], where larger roughness was observed in the aluminum version. It must be pointed out that the aluminum breadboard in [3] was subject to a sanding process, which is undoubtedly responsible for such roughness. As it is already suggested in [3], an eventual finishing process for aluminum pieces may lead to additional roughness which significantly increases the conductor losses. In our study, the ohmic losses are similar for both prototypes as it is evidenced from the measured antenna efficiency. Note that no finishing process has been applied here. On the other hand, 3D printing technique inherently avoids the typical rounded corners of milled structures, whose effect can be easily considered and corrected in simulation.

Regardless of antenna losses, the greater building fidelity perceived for the milled antenna is manifested in its electrical performance. Directivity values in Tables I and II and radiation patterns in Fig. 5 evidence a slightly better radiation performance of the aluminum antenna with respect to the 3D-printed version. This subtle difference is witnessed in H-plane radiation pattern, whose beamwidth is slightly narrower for the CNC-machined antenna. This fact is aggravated at the lower end of the operating band, probably owing to fabrication inaccuracies in the corporate feeding waveguides. The matching behavior in Fig. 6 also confirms the higher accuracy of the CNC machining technique when comparing with the simulated curve.

Another important aspect for comparison is the fabrication cost, either in terms of time or money. In regard to the price, the piece made of aluminum was roughly 3.5 times more expensive than the same piece in SLA 3D printing. Concerning manufacturing time, unfortunately, the external company did not provide the number of hours needed to manufacture the 3D piece. In this regard, a good reference might be the figure given in [3], where the machined breadboard took 5 times as long as the 3D-printed piece. Lastly, the 3D-printed antenna was 50% lighter than the aluminum version, making it very appealing for exigent weight specifications.

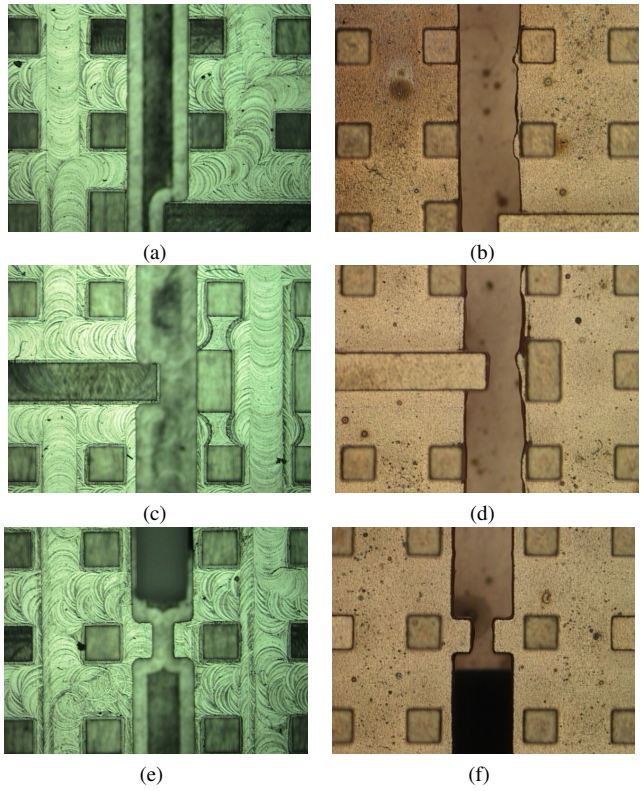

Fig. 7: Zoomed sampled views of the prototypes: (a), (c), (e) aluminum antenna; (b), (d), (f) 3D-printed antenna.

V. Conclusions

SLA additive manufacturing and CNC milling were assessed by comparing two instances of the same GW array antenna in Ka band. The electrical performance of the 3D-printed antenna has been slightly worse due to several fabrication inconsistencies. In that sense, the current 3D-printing accuracy is still not good enough to blindly trust on this technology for high-performance Ka-band antennas. Nonetheless, overall performance of the 3D-printed instance can be considered reasonably similar to that achieved by the accurately milled version. The used SLA 3D printing technique, hence, can be considered as a viable solution for low cost manufacturing of GW array antennas at Ka band, becoming very appealing in terms of fabrication time, cost and weight.

VI. Acknowledgements

This work has been supported by the Spanish Ministry of Economy and Competitiveness (Ministerio de Economía y Competitividad) under the project TEC2016-79700-C2-1-R.

REFERENCES

[1] E. Feltrin and E. Weller, "New frontiers for the mobile satellite interactive services," in *Advanced satellite multimedia systems conference (asma) and the 11th signal processing for space communications workshop (spsc), 2010 5th*. IEEE, 2010, pp. 155–161.

[2] P. S. Kildal, E. Alfonso, A. Valero-Nogueira, and E. Rajo-Iglesias, "Local Metamaterial-Based Waveguides in Gaps Between Parallel Metal Plates," *IEEE Antennas and Wireless Propagation Letters*, vol. 8, pp. 84–87, 2009.

[3] A. Tamayo-Domínguez, J.-M. Fernández-González, and M. Sierra-Pérez, "Groove gap waveguide in 3-D printed technology for low loss, weight, and cost distribution networks," *IEEE Transactions on Microwave Theory and Techniques*, vol. 65, no. 11, pp. 4138–4147, 2017.

[4] A. J. Sáez, A. Valero-Nogueira, J. I. Herranz, and B. Bernardo, "Single-layer cavity-backed slot array fed by groove gap waveguide," *IEEE Antennas and Wireless Propagation Letters*, vol. 15, pp. 1402–1405, 2016.

[5] M. Ferrando-Rocher, A. Valero-Nogueira, and J. I. Herranz-Herruzo, "New feeding network topologies for high-gain single-layer slot array antennas using gap waveguide concept," in *Antennas and Propagation (EUCAP), 2017 11th European Conference on*. IEEE, 2017, pp. 1654–1657.

[6] C. Guo, X. Shang, M. J. Lancaster, and J. Xu, "A 3-D printed lightweight X-band waveguide filter based on spherical resonators," *IEEE Microwave and Wireless Components Letters*, vol. 25, no. 7, pp. 442–444, 2015.

[7] G. P. Le Sage, "3D printed waveguide slot array antennas," *IEEE Access*, vol. 4, pp. 1258–1265, 2016.